

## Electronic Supplementary Information

### Amplification of Dissymmetry Factors by Dihedral Angle Engineering in Donor–Acceptor Type Circularly Polarized Luminescence Materials

Xing-Yu Chen,<sup>a</sup> Ji-Kun Li,<sup>a</sup> Wen-Long Zhao,<sup>b</sup> Cheng-Zhuo Du,<sup>a</sup> Meng Li,<sup>b</sup> Chuan-Feng Chen<sup>b</sup> and  
Xiao-Ye Wang<sup>\*a,c</sup>

---

<sup>a</sup> State Key Laboratory of Elemento-Organic Chemistry, College of Chemistry, Nankai University, Tianjin 300071 (China)

E-mail: xiaoye.wang@nankai.edu.cn

Homepage: <http://wang.nankai.edu.cn>.

<sup>b</sup> Beijing National Laboratory for Molecular Sciences, CAS Key Laboratory of Molecular Recognition and Function, Institute of Chemistry, Chinese Academy of Sciences, Beijing 100190 (China)

<sup>c</sup> State Key Laboratory of Luminescent Materials and Devices, South China University of Technology, Guangzhou 510640 (China)

## Table of Contents

### 1. General Methods

### 2. Synthetic Procedures

### 3. Optical Resolution and Chiroptical Properties

### 4. Electrochemical Properties

### 5. Theoretical Calculations

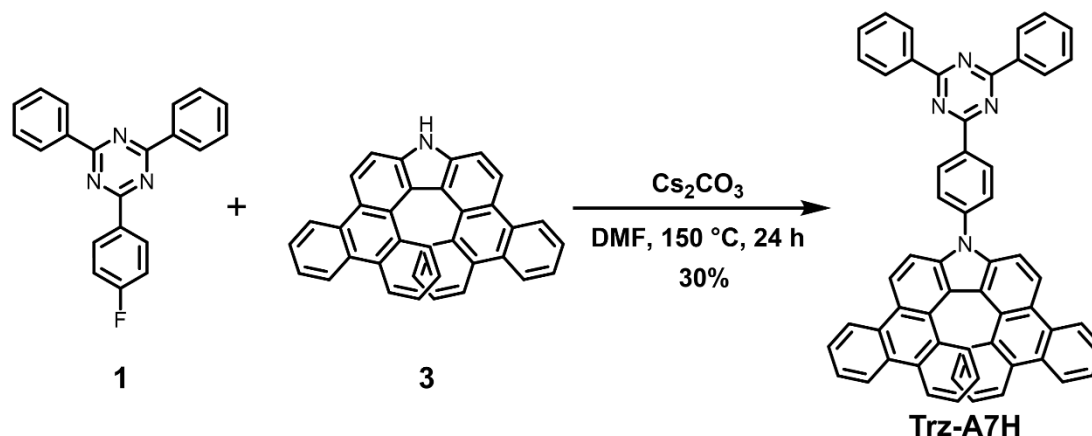
### 6. NMR Spectra

### 7. References

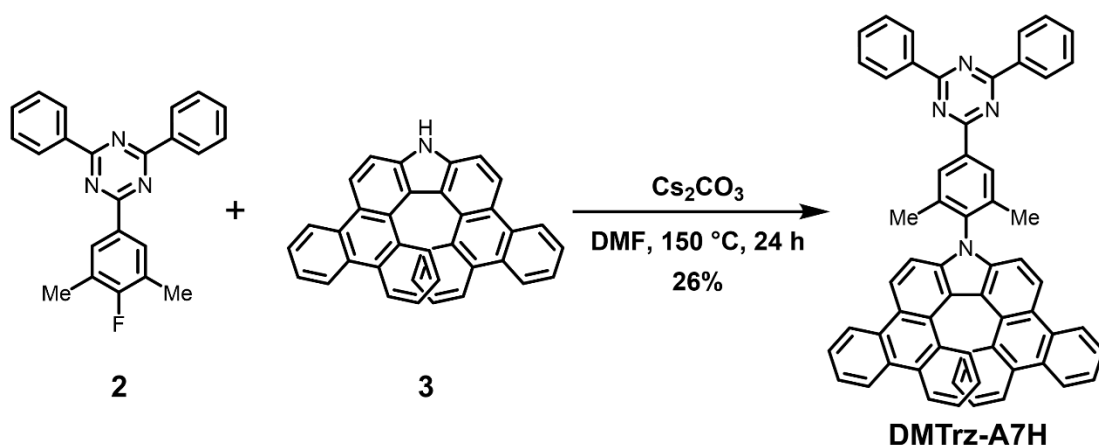
## 1. General Methods

All commercial materials were purchased from Bide Pharmatech, J&K Scientific and Heowns, and used as received without further purification unless otherwise noted. Anhydrous *N,N*-dimethylformamide (DMF) was purchased from J&K scientific. All reactions were carried out under argon atmosphere using Schlenk lines. Thin layer chromatography (TLC) plates and silica gel used for column chromatography were purchased from Yantai Xincheng with a grain size of 0.063-0.200 mm. Nuclear magnetic resonance (NMR) spectra were recorded in CD<sub>2</sub>Cl<sub>2</sub> on AVANCE 400 MHz Bruker spectrometers. <sup>1</sup>H NMR chemical shifts were referenced to CHDCl<sub>2</sub> (5.320 ppm). <sup>13</sup>C NMR chemical shifts were referenced to CD<sub>2</sub>Cl<sub>2</sub> (54.00 ppm). High-resolution mass spectrometry (HRMS) was performed on Agilent 6545B by electron spray ionization (ESI). UV-vis absorption spectra were recorded on an Analytikjena Specord 210 Plus UV-vis spectrophotometer. Photoluminescence spectra were recorded on an Edinburgh FSL1000 Spectrofluorometer. Photoluminescence quantum yields (PLQYs) were measured by an integrating sphere in toluene (*c* = 3.0 × 10<sup>-6</sup> M). Chiral high-performance liquid chromatography (HPLC) was implemented on a Daicel Chiralpak IE column. Circular dichroism (CD) spectra were collected on JASCO-810 circular dichroism spectrometer at 297 K. Circularly polarized luminescence (CPL) measurements were performed using JASCO CPL-300 at 297 K. Cyclic voltammogram (CV) was performed under argon atmosphere by CHI 620E electrochemical analyzer with the scan rate of 100 mV s<sup>-1</sup> (working electrode: glassy carbon, reference electrode: Ag/AgCl, counter electrode: platinum wire).

## 2. Synthetic Procedures



**Trz-A7H.** To a Schlenk flask under argon was added **1** (164 mg, 0.500 mmol), **3**<sup>1</sup> (222 mg, 0.480 mmol),  $\text{Cs}_2\text{CO}_3$  (814 mg, 2.50 mmol), and DMF (5 mL). The reaction mixture was then heated to  $150\text{ }^\circ\text{C}$  and stirred for 24 h. After cooling down to room temperature, the mixture was poured into brine and washed with MeOH. The residue was collected and purified by column chromatography over silica gel (eluent: petroleum ether/DCM = 3 : 1) and recrystallization from DCM/hexane to give 109 mg (yield: 30%) of **Trz-A7H** as a green solid.  $^1\text{H}$  NMR (400 MHz,  $\text{CD}_2\text{Cl}_2/\text{CS}_2$ , 297 K, ppm)  $\delta$  9.26 – 9.20 (m, 2H), 8.94 – 8.85 (m, 4H), 8.82 (d,  $J = 8.9$  Hz, 2H), 8.71 (dd,  $J = 11.0, 7.8$  Hz, 4H), 8.44 (d,  $J = 8.1$  Hz, 2H), 8.13 – 8.03 (m, 2H), 7.97 (d,  $J = 8.8$  Hz, 2H), 7.87 (dd,  $J = 8.2, 1.3$  Hz, 2H), 7.78 – 7.61 (m, 10H), 7.24 (m, 2H), 6.40 (m, 2H).  $^{13}\text{C}$  NMR (101 MHz,  $\text{CD}_2\text{Cl}_2/\text{CS}_2$ , 297 K, ppm)  $\delta$  172.40, 171.38, 141.40, 141.34, 136.77, 136.68, 133.38, 131.58, 131.22, 131.11, 129.95, 129.76, 129.37, 129.11, 128.84, 128.36, 128.30, 127.86, 127.59, 126.78, 125.47, 125.30, 124.28, 123.87, 122.53, 122.42, 119.57, 111.01. HRMS (ESI)  $m/z$ : Calcd. for  $\text{C}_{57}\text{H}_{35}\text{N}_4$ : 775.2862; found: 775.2853  $[\text{M} + \text{H}]^+$ .



**DMTrz-A7H.** To a Schlenk flask under argon was added **2** (40 mg, 0.11 mmol), **3** (50 mg, 0.10 mmol),  $\text{Cs}_2\text{CO}_3$  (179 mg, 0.550 mmol), and DMF (1 mL). The reaction mixture was then heated to 150 °C and stirred for 24 h. After cooling down to room temperature, the mixture was poured into brine and washed with MeOH. The residue was collected and purified by column chromatography over silica gel (eluent: petroleum ether/DCM = 3 : 1) and recrystallization from DCM/hexane to give 21 mg (yield: 26%) of **Trz-A7H** as a green solid.  $^1\text{H}$  NMR (400 MHz,  $\text{CD}_2\text{Cl}_2$ , 297 K, ppm)  $\delta$  8.94 – 8.79 (m, 8H), 8.78 – 8.71 (m, 4H), 8.50 (d,  $J$  = 8.4 Hz, 2H), 7.96 (dd,  $J$  = 8.2, 1.3 Hz, 2H), 7.78 – 7.62 (m, 10H), 7.53 (d,  $J$  = 8.8 Hz, 2H), 7.30 – 7.22 (m, 2H), 6.45 – 6.36 (m, 2H), 2.21 (s, 6H).  $^{13}\text{C}$  NMR (101 MHz,  $\text{CD}_2\text{Cl}_2$ , 297 K, ppm)  $\delta$  172.46, 171.96, 140.85, 139.64, 138.89, 137.67, 136.75, 133.33, 131.31, 131.12, 129.99, 129.79, 129.55, 129.34, 129.08, 128.66, 128.43, 127.74, 127.41, 126.52, 125.06, 124.97, 124.10, 123.77, 122.41, 122.35, 118.89, 110.66, 18.33. HRMS (ESI)  $m/z$ : Calcd. for  $\text{C}_{59}\text{H}_{39}\text{N}_4$ : 803.3175; found: 803.3172  $[\text{M} + \text{H}]^+$ .

### 3. Optical Resolution and Chiroptical Properties

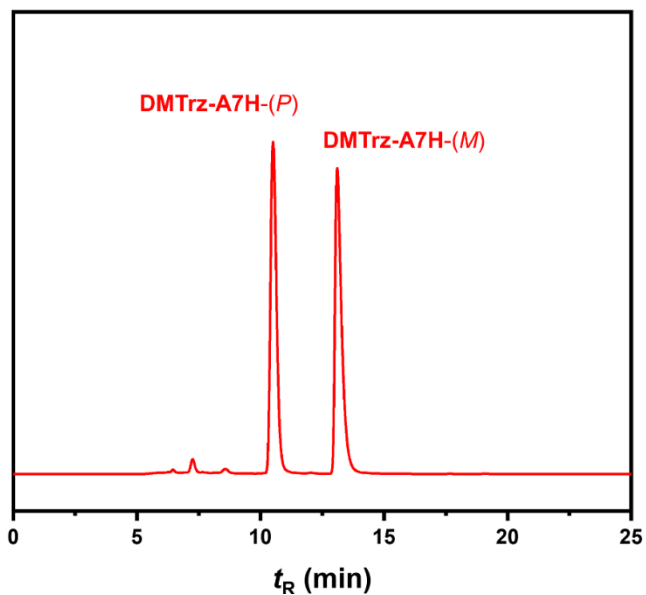


**Figure S1.** Chiral HPLC analysis of **DMTrz-A7H** eluted by DCM/hexane = 1 : 1 using Daicel Chiralpak IE column. Elution rate:  $0.5 \text{ mL} \cdot \text{min}^{-1}$ . The integration areas of the (*P*) and (*M*)- enantiomers are 49.7% and 50.3%, respectively.

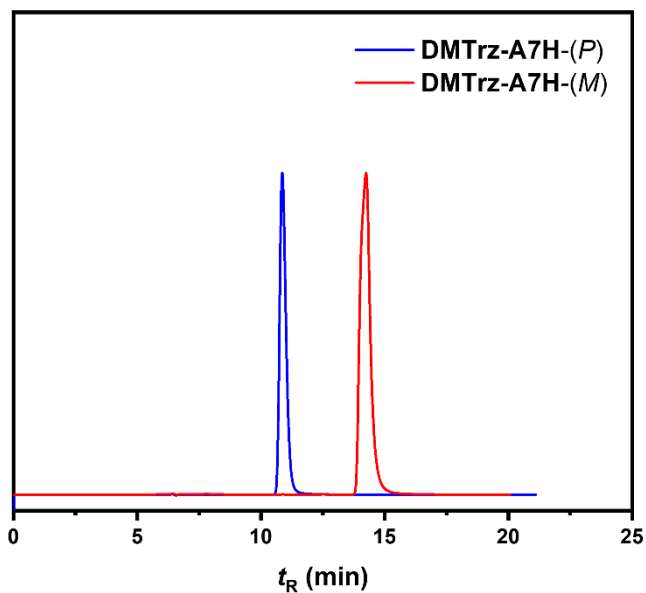


**Figure S2.** Chiral HPLC traces of the separated (*P*)- and (*M*)- enantiomers of **DMTrz-A7H** eluted by DCM/hexane = 1 : 1 using Daicel Chiralpak IE column. Elution rate:  $0.5 \text{ mL} \cdot \text{min}^{-1}$ .

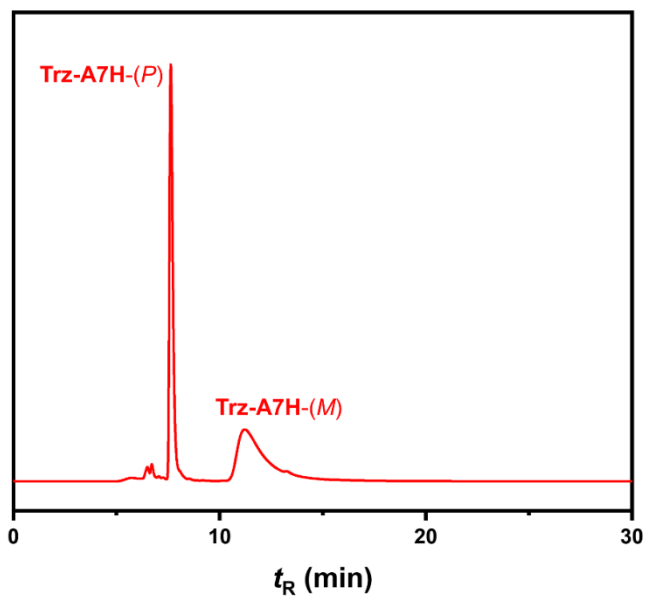


**Figure S3.** Chiral HPLC analysis of **Trz-A7H** eluted by DCM using Daicel Chiralpak IE column. Elution rate:  $0.5 \text{ mL}\cdot\text{min}^{-1}$ . The integration areas of the (*P*) and (*M*)-enantiomers are 49.7% and 50.3%, respectively.

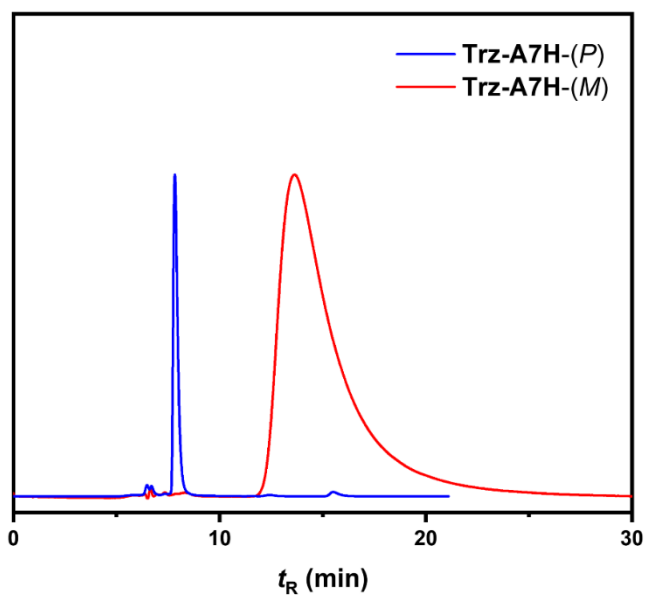


**Figure S4.** Chiral HPLC traces of the separated (*P*)- and (*M*)- enantiomers of **Trz-A7H** eluted by DCM using Daicel Chiralpak IE column. Elution rate:  $0.5 \text{ mL min}^{-1}$ .

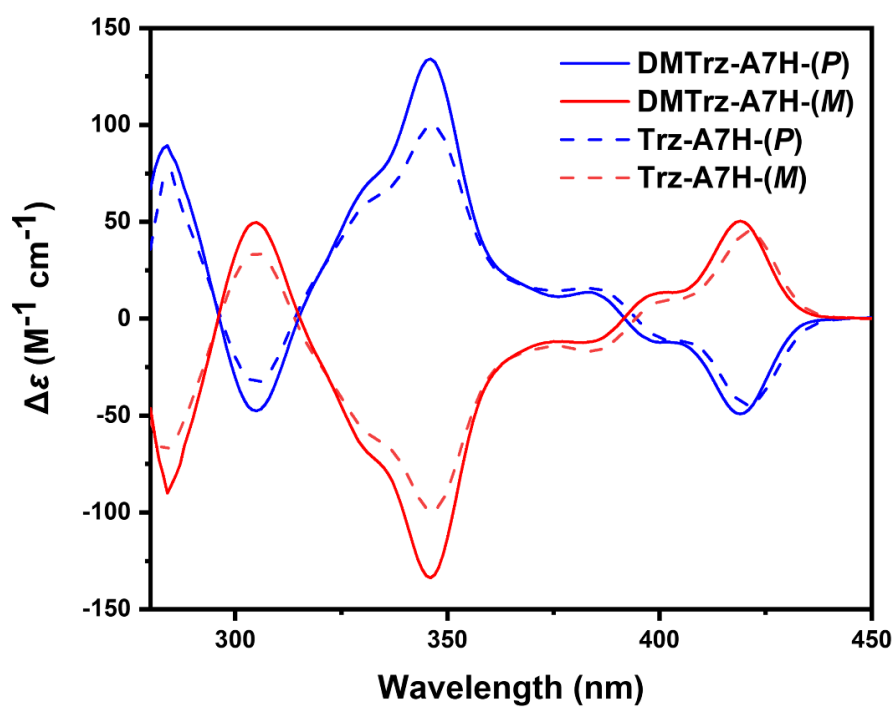


Figure S5. CD spectra of **DMTrz-A7H** and **Trz-A7H** in toluene ( $c = 1.0 \times 10^{-5}$  M).

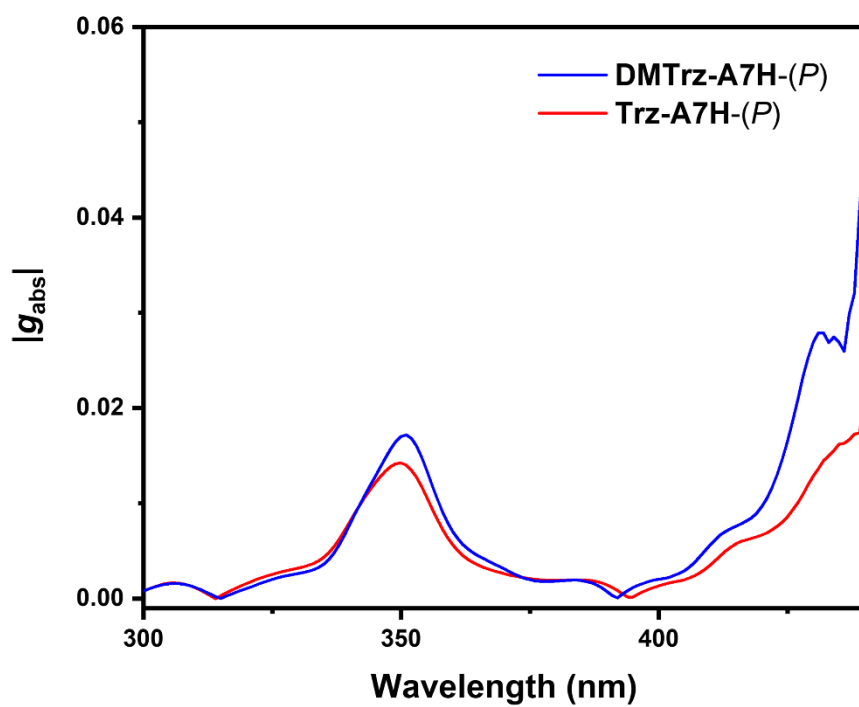
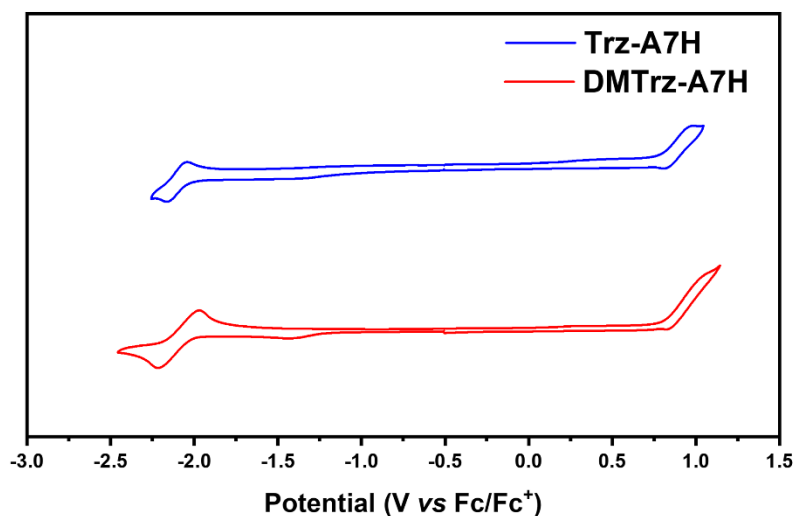


Figure S6. Absorption dissymmetry factors of **DMTrz-A7H** and **Trz-A7H** in toluene ( $c = 1.0 \times 10^{-5}$  M).

## 4. Electrochemical Properties



**Figure S7.** CV of **DMTrz-A7H** and **Trz-A7H** in tetrahydrofuran (1 mM) with 0.1 M *n*-Bu<sub>4</sub>NPF<sub>6</sub> as supporting electrolyte and ferrocene as an external standard.

## 5. Theoretical Calculations

Theoretical calculations were performed using the Gaussian 09 software package.<sup>2</sup> All calculations were carried out using the density functional theory (DFT) method. The ground-state and transition state (TS) geometries were optimized at the B3LYP/6-31G(d) level, and the excited-state geometries were optimized at the M06-2X/6-31G(d) level. The relative Gibbs free energy (kcal mol<sup>-1</sup>) was calculated at the B3LYP/def2TZVP level of theory. The rigid scanning was performed using the optimized geometries of **Trz-A7H** at the M06-2X/6-31G(d) level. The simulated UV-vis and CD spectra were calculated by time-dependent DFT (TD-DFT) at the CAM-B3LYP/6-31G(d) level. The transition electric and magnetic dipole moment vectors were calculated by Multiwfn<sup>3</sup> and rendered by VMD.<sup>4</sup> The transition electric dipole moment density (only for x-axis component) and the transition magnetic dipole moment density (only for x-axis component) were calculated by Multiwfn.



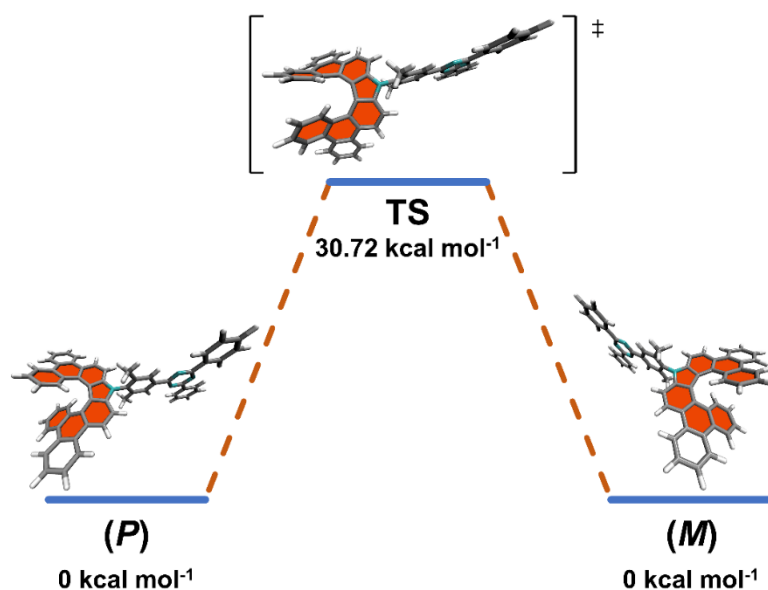


**Figure S8.** Enantiomerization process of **DMTrz-A7H** from (*P*)- to (*M*)-configuration. The relative Gibbs free energy at 298 K is calculated at the B3LYP/def2TZVP level.

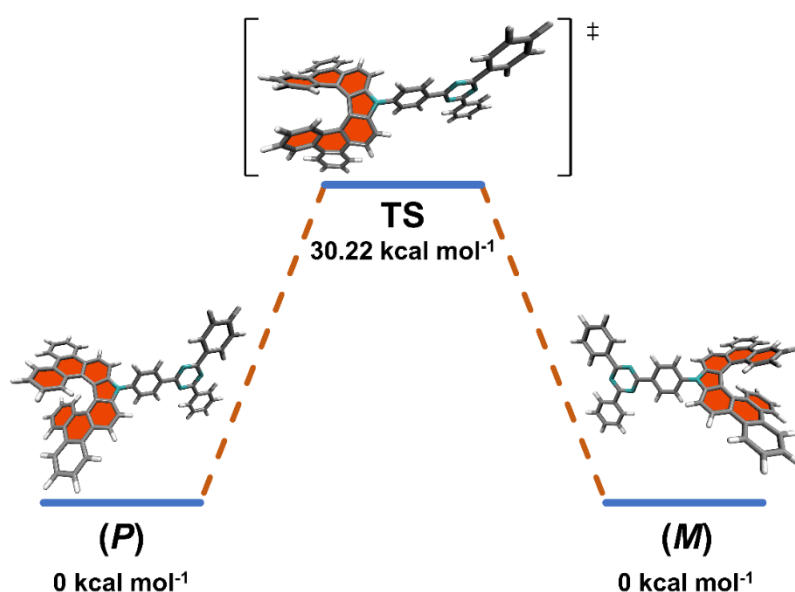


**Figure S9.** Enantiomerization process of **Trz-A7H** from (*P*)- to (*M*)-configuration. The relative Gibbs free energy at 298 K is calculated at the B3LYP/def2TZVP level.

The half-life ( $\tau_{1/2}$ ) of **DMTrz-A7H** and **Trz-A7H** is calculated by using the Gibbs free energy ( $\Delta G^\ddagger$ ) at room temperature (298 K) based on the Eyring equation<sup>5</sup>:

$$\Delta G^\ddagger(T) = -RT \ln(k_e h / \kappa k_B T) \quad (1)$$

where  $R$ ,  $T$ ,  $h$ ,  $k_e$ ,  $k_B$  are gas constant, absolute temperature, Planck's constant, rate constant, and Boltzmann constant, respectively. Parameter  $\kappa$  is assumed as 0.5.<sup>6</sup> The

enantiomerization process of **DMTrz-A7H** and **Trz-A7H** is a first-order reaction, so the following equation is adopted:

$$\tau_{1/2} = \ln 2 / k_e \quad (2)$$

The enantiomerization process of **DMTrz-A7H** and **Trz-A7H** shows  $\tau_{1/2}$  of  $7.58 \times 10^9$  s and  $3.25 \times 10^9$  s at room temperature, respectively, indicating their excellent chiral stability.

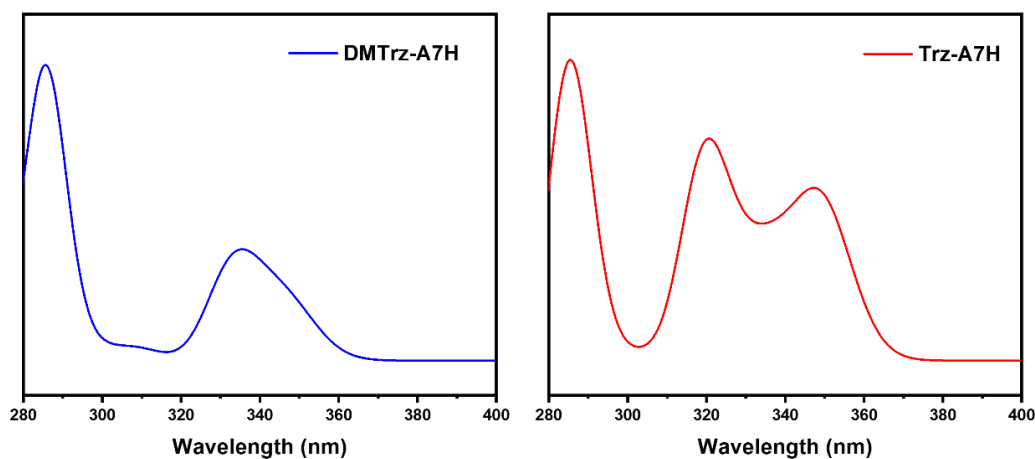


**Figure S10.** DFT-simulated UV-vis absorption spectra of **DMTrz-A7H** and **Trz-A7H** (FWHM =  $726 \text{ cm}^{-1}$ ).

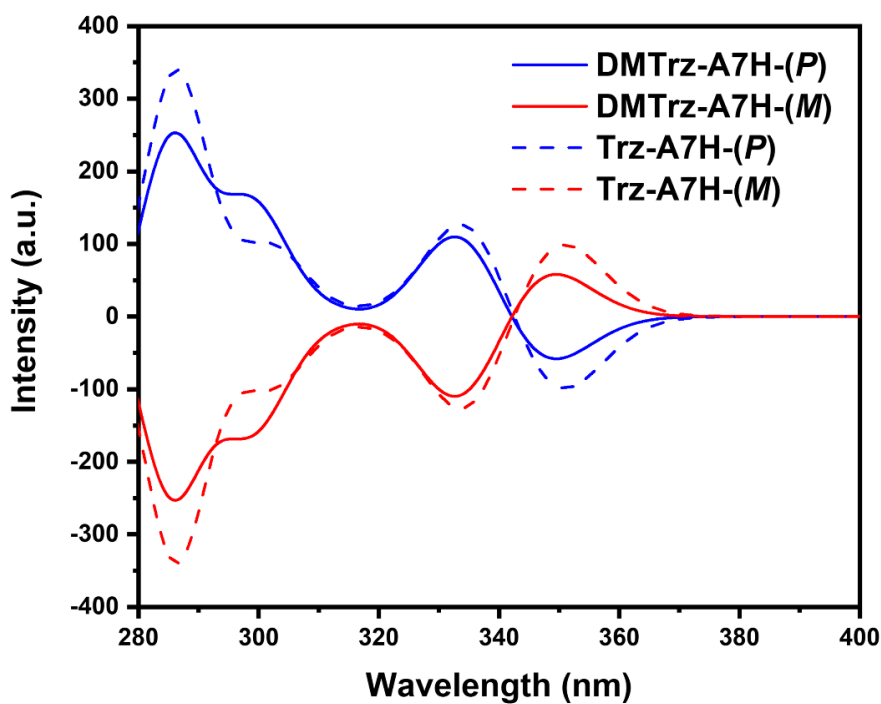


**Figure S11.** DFT-simulated CD spectra of **DMTrz-A7H** and **Trz-A7H** (FWHM= $726 \text{ cm}^{-1}$ ).

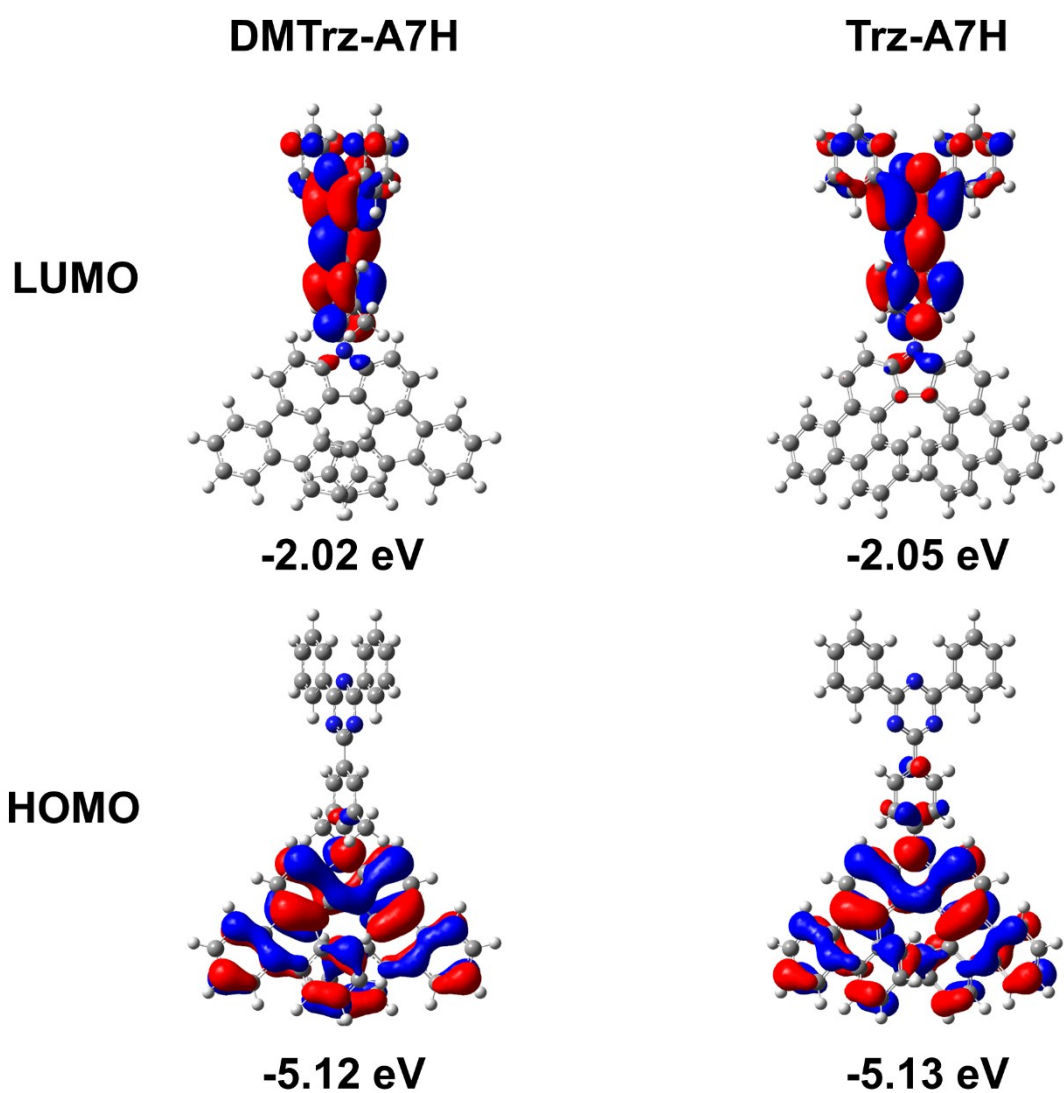


**Figure S12.** Frontier molecular orbitals of DMTrz-A7H and Trz-A7H at the optimized geometries of the  $S_0$  state (isoval = 0.02).

**Table S1.** Summary of the TD-DFT calculation results of DMTrz-A7H at the ground state geometry ( $S_0$ ).

Excited States <sup>a</sup>	Energy (eV)	Wavelength (nm)	Oscillator Strength	Major Contributions
$S_1$	3.5738	346.92	0.1058	HOMO-1 $\rightarrow$ LUMO+3 (9%) HOMO $\rightarrow$ LUMO (3%) HOMO $\rightarrow$ LUMO+2 (80%)

S <sub>2</sub>	3.7152	333.72	0.1909	HOMO-1→LUMO+2 (83%) HOMO→LUMO+3 (5%)
S <sub>3</sub>	4.0104	309.16	0.0220	HOMO→LUMO (82%) HOMO→LUMO+2 (2%) HOMO→LUMO+6 (2%)

<sup>a</sup>Only S<sub>1</sub> ~ S<sub>3</sub> have been displayed.

**Table S2.** Summary of the TD-DFT calculation results of **Trz-A7H** at the ground state geometry (S<sub>0</sub>).

Excited States <sup>a</sup>	Energy (eV)	Wavelength (nm)	Oscillator Strength	Major Contributions
S <sub>1</sub>	3.5512	349.14	0.2995	HOMO-1→LUMO+3 (7%) HOMO→LUMO (18%) HOMO→LUMO+2 (65%)
S <sub>2</sub>	3.7026	334.86	0.1891	HOMO-1→LUMO (5%) HOMO-1→LUMO+2 (80%) HOMO→LUMO+3 (5%)
S <sub>3</sub>	3.8740	320.04	0.4105	HOMO-6→LUMO (4%) HOMO-5→LUMO (3%) HOMO-1→LUMO+3 (2%) HOMO→LUMO (60%) HOMO→LUMO+2 (17%) HOMO→LUMO+5 (6%)

<sup>a</sup>Only S<sub>1</sub> ~ S<sub>3</sub> have been displayed.

**Table S3.** Summary of the TD-DFT calculation results of **DMTrz-A7H** at the first singlet excited state geometry (S<sub>1</sub>).

Excited States <sup>a</sup>	Energy (eV)	Wavelength (nm)	Oscillator Strength	Major Contributions
S <sub>1</sub>	3.3465	370.49	0.1686	HOMO-1→LUMO+3 (6%)

				HOMO→LUMO (20%)
				HOMO→LUMO+2 (68%)
S <sub>2</sub>	3.5539	348.87	0.2022	HOMO-1→LUMO (12%)
				HOMO-1→LUMO+2 (78%)
				HOMO→LUMO+3 (3%)
S <sub>3</sub>	3.8327	323.49	0.0761	HOMO→LUMO (68%)
				HOMO→LUMO+2 (19%)
				HOMO→LUMO+6 (3%)

<sup>a</sup>Only S<sub>1</sub> ~ S<sub>3</sub> have been displayed.

**Table S4.** Summary of the TD-DFT calculation results of **Trz-A7H** at the first singlet excited state geometry (S<sub>1</sub>).

Excited States <sup>a</sup>	Energy (eV)	Wavelength (nm)	Oscillator Strength	Major Contributions
S <sub>1</sub>	3.3365	371.60	0.3374	HOMO-1→LUMO+3 (6%)
				HOMO→LUMO (29%)
				HOMO→LUMO+2 (58%)
S <sub>2</sub>	3.5340	350.83	0.2057	HOMO-1→LUMO (12%)
				HOMO-1→LUMO+2 (79%)
				HOMO→LUMO+3 (3%)
S <sub>3</sub>	3.6997	335.12	0.4149	HOMO-6→LUMO (2%)
				HOMO-5→LUMO (3%)
				HOMO→LUMO (54%)
				HOMO→LUMO+2 (29%)
				HOMO→LUMO+5 (4%)

<sup>a</sup>Only S<sub>1</sub> ~ S<sub>3</sub> have been displayed.

### Cartesian coordinates obtained in gas-phase DFT calculations

The S<sub>0</sub> state geometry of **DMTrz-A7H-(P)**

Tag	Symbol	X	Y	Z
1	C	-7.238707	-0.090051	-1.134020
2	N	-5.896724	-0.093877	-1.182084
3	C	-5.270749	-0.000018	-0.000012
4	N	-5.896655	0.093818	1.182100
5	C	-7.238640	0.090110	1.134105
6	N	-7.950083	0.000089	0.000059
7	C	-7.980255	-0.192056	-2.413809
8	C	-3.785191	-0.000031	-0.000054
9	C	-7.980114	0.192069	2.413942
10	C	-9.384145	-0.191551	-2.422928
11	C	-10.079206	-0.287609	-3.625725
12	C	-9.382800	-0.385303	-4.832956
13	C	-7.985703	-0.386442	-4.831650
14	C	-7.287271	-0.290491	-3.630776
15	C	-9.384003	0.191962	2.423110
16	C	-10.078996	0.287982	3.625949
17	C	-9.382518	0.385216	4.833177
18	C	-7.985422	0.385943	4.831825
19	C	-7.287059	0.290054	3.630905
20	C	-3.077928	0.085474	1.205579
21	C	-1.682120	0.084963	1.227616
22	C	-0.998998	-0.000051	-0.000137
23	C	-1.682195	-0.085057	-1.227851
24	C	-3.077999	-0.085549	-1.205731
25	C	-0.927867	0.171554	2.533050
26	C	-0.928017	-0.171616	-2.533331
27	C	1.244997	-1.121679	0.038543
28	C	2.608224	-0.729130	0.087012
29	C	2.608211	0.729100	-0.087193
30	C	1.244970	1.121612	-0.038819
31	N	0.433188	-0.000046	-0.000183
32	C	0.830056	-2.458309	0.025963
33	C	1.810393	-3.426975	0.024499
34	C	3.184069	-3.106798	0.173098
35	C	3.577368	-1.752407	0.362370
36	C	3.577350	1.752405	-0.362471
37	C	3.184004	3.106782	-0.173197
38	C	1.810310	3.426921	-0.024692
39	C	0.829996	2.458231	-0.026250

40	C	4.206961	-4.155973	0.118577
41	C	5.551964	-3.856519	0.462241
42	C	5.864274	-2.539409	1.014166
43	C	4.890834	-1.503167	0.961212
44	C	4.890866	1.503211	-0.961226
45	C	5.864283	2.539479	-1.014084
46	C	5.551900	3.856569	-0.462151
47	C	4.206865	4.155982	-0.118580
48	C	7.092593	-2.283621	1.660600
49	C	7.357690	-1.066564	2.264378
50	C	6.377421	-0.065777	2.263106
51	C	5.169251	-0.288934	1.626794
52	C	5.169359	0.289006	-1.626827
53	C	6.377580	0.065898	-2.263060
54	C	7.357826	1.066709	-2.264232
55	C	7.092655	2.283741	-1.660438
56	C	3.907903	-5.457091	-0.345790
57	C	4.887203	-6.426624	-0.477852
58	C	6.217613	-6.121494	-0.159565
59	C	6.536486	-4.854748	0.298010
60	C	6.536386	4.854819	-0.297828
61	C	6.217448	6.121547	0.159750
62	C	4.887008	6.426638	0.477945
63	C	3.907740	5.457083	0.345791
64	H	-9.913986	-0.115333	-1.480392
65	H	-11.165809	-0.286338	-3.622330
66	H	-9.926624	-0.460221	-5.770970
67	H	-7.440236	-0.462229	-5.768372
68	H	-6.203410	-0.290487	-3.618012
69	H	-9.913900	0.116073	1.480578
70	H	-11.165599	0.287043	3.622593
71	H	-9.926289	0.460094	5.771226
72	H	-7.439901	0.461357	5.768545
73	H	-6.203198	0.289754	3.618103
74	H	-3.633756	0.149847	2.134203
75	H	-3.633885	-0.149914	-2.134321
76	H	-1.621696	0.206676	3.377611
77	H	-0.265740	-0.690755	2.670684
78	H	-0.296613	1.066797	2.573557
79	H	-0.296350	-1.066569	-2.573690
80	H	-1.621904	-0.207242	-3.377824
81	H	-0.266308	0.690976	-2.671222
82	H	-0.223718	-2.715671	-0.009500
83	H	1.506585	-4.465531	-0.028524

84	H	1.506471	4.465468	0.028333
85	H	-0.223787	2.715570	0.009144
86	H	7.836917	-3.069281	1.726944
87	H	8.309670	-0.904113	2.762657
88	H	6.554358	0.878935	2.769586
89	H	4.406120	0.476467	1.667008
90	H	4.406250	-0.476411	-1.667124
91	H	6.554576	-0.878795	-2.769557
92	H	8.309844	0.904296	-2.762450
93	H	7.836963	3.069422	-1.726709
94	H	2.896104	-5.703716	-0.646854
95	H	4.623969	-7.413682	-0.848427
96	H	6.997503	-6.868293	-0.280796
97	H	7.573744	-4.625561	0.516305
98	H	7.573665	4.625662	-0.516053
99	H	6.997311	6.868362	0.281053
100	H	4.623721	7.413682	0.848520
101	H	2.895913	5.703678	0.646785

The  $S_0$  state geometry of Trz-A7H-(P)

Tag	Symbol	X	Y	Z
1	C	-7.287887	0.897494	-0.699507
2	N	-5.945902	0.936266	-0.728578
3	C	-5.320553	-0.000002	-0.000006
4	N	-5.945892	-0.936273	0.728573
5	C	-7.287877	-0.897504	0.699516
6	N	-7.999081	-0.000006	0.000008
7	C	-8.029676	1.909735	-1.488817
8	C	-8.029655	-1.909748	1.488833
9	C	-3.837648	0.000001	-0.000012
10	C	-9.433565	1.912330	-1.499502
11	C	-10.128956	2.863698	-2.241359
12	C	-9.432927	3.823297	-2.980709
13	C	-8.035843	3.826983	-2.974756
14	C	-7.337093	2.877025	-2.234231
15	C	-9.433544	-1.912332	1.499552
16	C	-10.128924	-2.863703	2.241416
17	C	-9.432885	-3.823315	2.980738
18	C	-8.035801	-3.827013	2.974751
19	C	-7.337061	-2.877051	2.234219
20	C	-3.123955	-0.936295	0.763872
21	C	-1.733641	-0.933554	0.772039
22	C	-1.028400	0.000006	-0.000025



23	C	-1.733652	0.933563	-0.772082
24	C	-3.123965	0.936299	-0.763903
25	C	1.208070	-1.091896	-0.272879
26	C	2.568151	-0.724593	-0.115632
27	C	2.568150	0.724604	0.115612
28	C	1.208066	1.091912	0.272833
29	N	0.390850	0.000009	-0.000032
30	C	0.809386	-2.362761	-0.705150
31	C	1.797849	-3.280144	-0.986807
32	C	3.166930	-3.017047	-0.726849
33	C	3.546221	-1.776335	-0.145244
34	C	3.546221	1.776345	0.145237
35	C	3.166923	3.017062	0.726827
36	C	1.797839	3.280163	0.986761
37	C	0.809378	2.362780	0.705093
38	C	4.198514	-4.000437	-1.071750
39	C	5.539101	-3.802997	-0.646257
40	C	5.837609	-2.698938	0.264172
41	C	4.854814	-1.699544	0.507685
42	C	4.854824	1.699544	-0.507670
43	C	5.837618	2.698938	-0.264151
44	C	5.539098	3.803006	0.646264
45	C	4.198505	4.000451	1.071736
46	C	7.061439	-2.631114	0.964108
47	C	7.313148	-1.638497	1.895343
48	C	6.323460	-0.688072	2.178073
49	C	5.119289	-0.727745	1.498011
50	C	5.119311	0.727732	-1.497979
51	C	6.323493	0.688047	-2.178021
52	C	7.313179	1.638473	-1.895287
53	C	7.061458	2.631102	-0.964067
54	C	3.913111	-5.116487	-1.890895
55	C	4.901582	-6.000088	-2.288902
56	C	6.227799	-5.789165	-1.887605
57	C	6.533178	-4.705089	-1.083266
58	C	6.533170	4.705098	1.083281
59	C	6.227783	5.789181	1.887609
60	C	4.901560	6.000109	2.288886
61	C	3.913093	5.116507	1.890870
62	H	-9.963095	1.163174	-0.922211
63	H	-11.215540	2.857329	-2.243361
64	H	-9.977038	4.565254	-3.559207
65	H	-7.490647	4.571597	-3.548350
66	H	-6.253243	2.870811	-2.222332

67	H	-9.963082	-1.163166	0.922282
68	H	-11.215508	-2.857324	2.243446
69	H	-9.976988	-4.565276	3.559239
70	H	-7.490597	-4.571638	3.548323
71	H	-6.253211	-2.870845	2.222295
72	H	-3.674104	-1.654179	1.361037
73	H	-1.186213	-1.642202	1.385184
74	H	-1.186231	1.642213	-1.385232
75	H	-3.674123	1.654181	-1.361062
76	H	-0.237828	-2.604008	-0.849732
77	H	1.501118	-4.251640	-1.362994
78	H	1.501103	4.251662	1.362937
79	H	-0.237837	2.604030	0.849655
80	H	7.812999	-3.396245	0.804931
81	H	8.261957	-1.619393	2.424787
82	H	6.489859	0.070951	2.937337
83	H	4.348687	-0.013241	1.754158
84	H	4.348712	0.013224	-1.754126
85	H	6.489902	-0.070986	-2.937273
86	H	8.261997	1.619359	-2.424715
87	H	7.813019	3.396231	-0.804886
88	H	2.904791	-5.275634	-2.255555
89	H	4.648688	-6.841656	-2.928169
90	H	7.014887	-6.464092	-2.212552
91	H	7.567267	-4.541146	-0.800815
92	H	7.567263	4.541153	0.800845
93	H	7.014867	6.464108	2.212563
94	H	4.648659	6.841681	2.928144
95	H	2.904768	5.275659	2.255514

The  $S_1$  state geometry of **DMTrz-A7H-(P)**

Tag	Symbol	X	Y	Z
1	C	-7.211191	-0.550785	0.988047
2	N	-5.876228	-0.574418	1.033244
3	C	-5.253932	0.000102	0.000056
4	N	-5.876210	0.574581	-1.033165
5	C	-7.211174	0.550922	-0.988005
6	N	-7.922234	0.000053	0.000006
7	C	-7.953376	-1.178689	2.108206
8	C	-3.771386	0.000075	0.000054
9	C	-7.953339	1.178743	-2.108224
10	C	-9.351431	-1.170646	2.115801
11	C	-10.045483	-1.760496	3.165385

12	C	-9.350178	-2.361885	4.212603
13	C	-7.956660	-2.371840	4.208119
14	C	-7.258960	-1.782664	3.160644
15	C	-9.351393	1.170629	-2.115883
16	C	-10.045427	1.760404	-3.165521
17	C	-9.350104	2.361788	-4.212730
18	C	-7.956587	2.371811	-4.208184
19	C	-7.258905	1.782710	-3.160654
20	C	-3.070716	0.546806	-1.077920
21	C	-1.679885	0.554407	-1.099336
22	C	-1.006627	0.000029	0.000049
23	C	-1.679900	-0.554329	1.099434
24	C	-3.070731	-0.546683	1.078023
25	C	-0.914370	1.124263	-2.263782
26	C	-0.914395	-1.124219	2.263870
27	C	1.210011	1.109213	0.204341
28	C	2.579824	0.720227	0.071516
29	C	2.579812	-0.720234	-0.071441
30	C	1.209968	-1.109191	-0.204244
31	N	0.417498	0.000006	0.000051
32	C	0.786228	2.391593	0.530497
33	C	1.774294	3.345283	0.774748
34	C	3.135309	3.051501	0.583309
35	C	3.540798	1.773287	0.047555
36	C	3.540761	-1.773312	-0.047483
37	C	3.135232	-3.051501	-0.583261
38	C	1.774188	-3.345263	-0.774674
39	C	0.786148	-2.391580	-0.530393
40	C	4.178207	4.003015	0.955385
41	C	5.527045	3.771759	0.582101
42	C	5.855440	2.625882	-0.269619
43	C	4.855307	1.652946	-0.535406
44	C	4.855297	-1.653004	0.535434
45	C	5.855400	-2.625950	0.269580
46	C	5.526951	-3.771787	-0.582165
47	C	4.178088	-4.003011	-0.955406
48	C	7.122674	2.465458	-0.845040
49	C	7.415275	1.391918	-1.673903
50	C	6.415148	0.467157	-1.985404
51	C	5.154977	0.606820	-1.437473
52	C	5.155022	-0.606919	1.437524
53	C	6.415219	-0.467303	1.985415
54	C	7.415318	-1.392071	1.673848
55	C	7.122661	-2.465575	0.844962

56	C	3.881211	5.130359	1.750826
57	C	4.864149	6.008727	2.160690
58	C	6.194079	5.773663	1.797804
59	C	6.511985	4.668794	1.028785
60	C	6.511857	-4.668827	-1.028916
61	C	6.193902	-5.773667	-1.797954
62	C	4.863951	-6.008701	-2.160797
63	C	3.881045	-5.130334	-1.750871
64	H	-9.877909	-0.698987	1.293661
65	H	-11.130900	-1.751700	3.167220
66	H	-9.893895	-2.822701	5.031707
67	H	-7.413371	-2.840193	5.022771
68	H	-6.174853	-1.782932	3.142654
69	H	-9.877885	0.698976	-1.293748
70	H	-11.130843	1.751554	-3.167406
71	H	-9.893807	2.822545	-5.031877
72	H	-7.413284	2.840160	-5.022829
73	H	-6.174799	1.783033	-3.142615
74	H	-3.628235	0.961280	-1.911274
75	H	-3.628260	-0.961141	1.911378
76	H	-1.585904	1.324760	-3.101084
77	H	-0.414745	2.060224	-1.989454
78	H	-0.135414	0.431661	-2.598558
79	H	-0.135424	-0.431639	2.598654
80	H	-1.585933	-1.324714	3.101171
81	H	-0.414792	-2.060188	1.989526
82	H	-0.269848	2.618228	0.637797
83	H	1.471622	4.335302	1.089788
84	H	1.471505	-4.335280	-1.089711
85	H	-0.269935	-2.618193	-0.637665
86	H	7.896171	3.203603	-0.665403
87	H	8.408318	1.293105	-2.100292
88	H	6.618210	-0.354408	-2.665422
89	H	4.369710	-0.083910	-1.718891
90	H	4.369783	0.083818	1.719000
91	H	6.618320	0.354236	2.665453
92	H	8.408378	-1.293293	2.100205
93	H	7.896132	-3.203735	0.665275
94	H	2.863923	5.298098	2.083854
95	H	4.605868	6.862792	2.778415
96	H	6.979473	6.446158	2.128266
97	H	7.552249	4.491363	0.782082
98	H	7.552134	-4.491422	-0.782249
99	H	6.979272	-6.446166	-2.128467

100	H	4.605635	-6.862745	-2.778538
101	H	2.863742	-5.298048	-2.083867

The S<sub>1</sub> state geometry of **Trz-A7H-(P)**

Tag	Symbol	X	Y	Z
1	C	-7.266350	0.931491	-0.642613
2	N	-5.932259	0.974008	-0.672571
3	C	-5.309189	-0.000015	0.000009
4	N	-5.932269	-0.974037	0.672580
5	C	-7.266360	-0.931518	0.642604
6	N	-7.978184	-0.000013	-0.000010
7	C	-8.009386	1.989292	-1.370223
8	C	-8.009407	-1.989318	1.370204
9	C	-3.832819	-0.000015	0.000020
10	C	-9.407469	1.987814	-1.375550
11	C	-10.102513	2.979916	-2.056890
12	C	-9.408267	3.978943	-2.736423
13	C	-8.014663	3.983547	-2.733171
14	C	-7.316126	2.993178	-2.053215
15	C	-9.407491	-1.987838	1.375512
16	C	-10.102545	-2.979938	2.056844
17	C	-9.408309	-3.978965	2.736388
18	C	-8.014706	-3.983571	2.733155
19	C	-7.316158	-2.993204	2.053207
20	C	-3.123714	-0.966901	0.725755
21	C	-1.739419	-0.971618	0.728517
22	C	-1.039263	-0.000016	0.000040
23	C	-1.739408	0.971589	-0.728444
24	C	-3.123703	0.966872	-0.725704
25	C	1.171543	-1.113031	-0.205368
26	C	2.539734	-0.718543	-0.068689
27	C	2.539721	0.718547	0.068819
28	C	1.171524	1.113026	0.205451
29	N	0.368999	-0.000011	0.000052
30	C	0.772762	-2.389417	-0.583203
31	C	1.770744	-3.328675	-0.835102
32	C	3.126743	-3.034044	-0.609979
33	C	3.511069	-1.763964	-0.051260
34	C	3.511040	1.763976	0.051347
35	C	3.126691	3.034103	0.609942
36	C	1.770686	3.328725	0.835040
37	C	0.772722	2.389427	0.583212
38	C	4.181281	-3.976650	-0.975202

39	C	5.523916	-3.735797	-0.588355
40	C	5.833507	-2.593342	0.273936
41	C	4.820959	-1.635010	0.542767
42	C	4.820938	1.634961	-0.542635
43	C	5.833470	2.593341	-0.273918
44	C	5.523855	3.735898	0.588231
45	C	4.181216	3.976767	0.975061
46	C	7.095325	-2.423965	0.859810
47	C	7.368603	-1.356899	1.702425
48	C	6.355114	-0.447751	2.017909
49	C	5.101475	-0.595617	1.458312
50	C	5.101492	0.595398	-1.457974
51	C	6.355144	0.447457	-2.017518
52	C	7.368608	1.356685	-1.702178
53	C	7.095299	2.423887	-0.859743
54	C	3.901301	-5.102794	-1.778180
55	C	4.895924	-5.969330	-2.184716
56	C	6.220621	-5.723941	-1.809467
57	C	6.521448	-4.621240	-1.031184
58	C	6.521372	4.621406	1.030966
59	C	6.220527	5.724186	1.809130
60	C	4.895827	5.969592	2.184354
61	C	3.901219	5.102993	1.777917
62	H	-9.933158	1.203897	-0.841995
63	H	-11.187976	2.974566	-2.058259
64	H	-9.952768	4.753344	-3.268210
65	H	-7.471940	4.760840	-3.261876
66	H	-6.231994	2.983711	-2.041199
67	H	-9.933171	-1.203921	0.841948
68	H	-11.188008	-2.974587	2.058198
69	H	-9.952819	-4.753365	3.268168
70	H	-7.471991	-4.760864	3.261869
71	H	-6.232026	-2.983738	2.041207
72	H	-3.677538	-1.704533	1.295331
73	H	-1.185921	-1.701998	1.309716
74	H	-1.185901	1.701973	-1.309630
75	H	-3.677518	1.704505	-1.295286
76	H	-0.273313	-2.631845	-0.731196
77	H	1.476567	-4.310357	-1.181677
78	H	1.476489	4.310431	1.181529
79	H	-0.273360	2.631851	0.731168
80	H	7.879040	-3.150434	0.677466
81	H	8.357405	-1.250800	2.136917
82	H	6.543428	0.367838	2.709215

83	H	4.306105	0.082934	1.741144
84	H	4.306142	-0.083239	-1.740670
85	H	6.543492	-0.368255	-2.708669
86	H	8.357422	1.250525	-2.136628
87	H	7.879006	3.150388	-0.677491
88	H	2.888591	-5.280757	-2.119349
89	H	4.650674	-6.822744	-2.808597
90	H	7.014916	-6.387372	-2.136908
91	H	7.557692	-4.436233	-0.773594
92	H	7.557620	4.436386	0.773400
93	H	7.014811	6.387666	2.136499
94	H	4.650564	6.823069	2.808144
95	H	2.888506	5.280973	2.119071

---

## 6. NMR Spectra

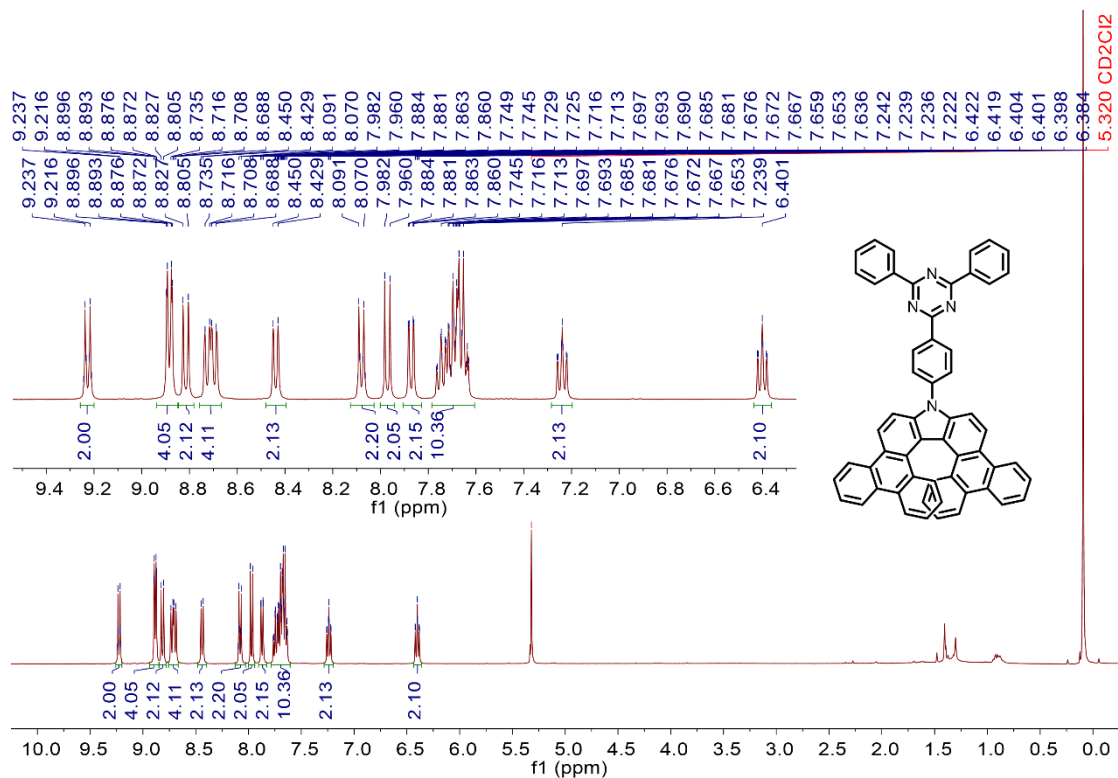


**Figure S13. <sup>1</sup>H NMR spectrum of Trz-A7H (400 MHz, CD<sub>2</sub>Cl<sub>2</sub>/CS<sub>2</sub>, 297 K).**

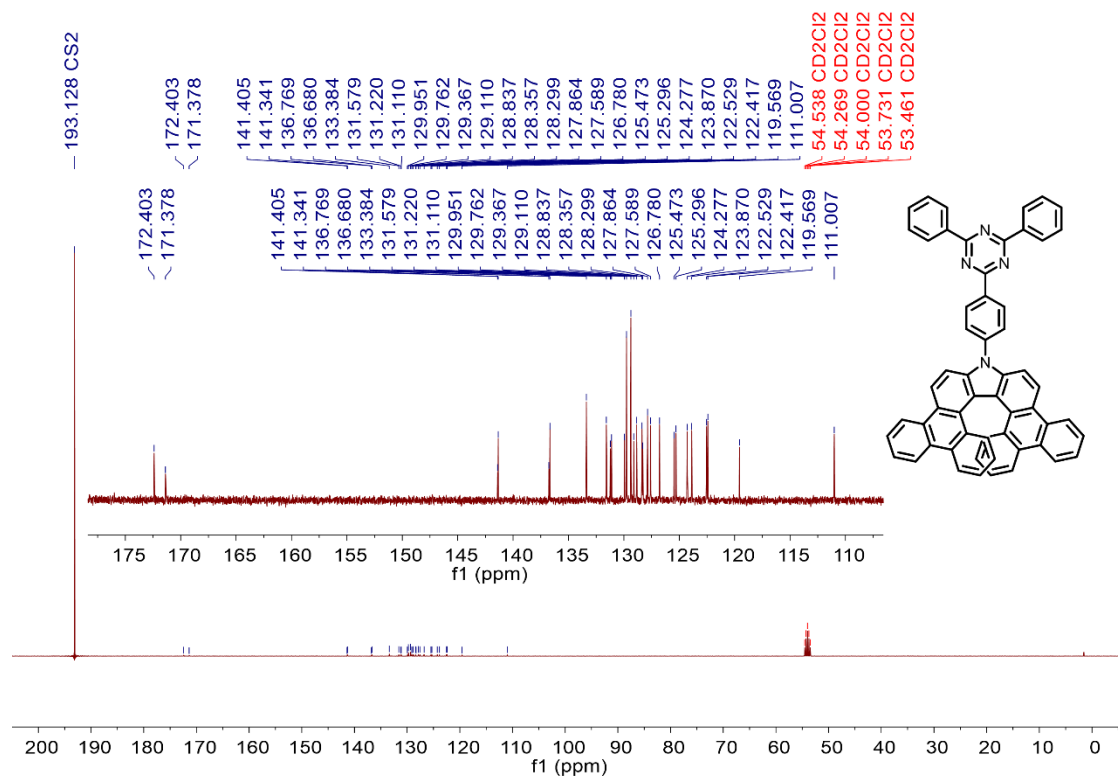


**Figure S14. <sup>13</sup>C NMR spectrum of Trz-A7H (101 MHz, CD<sub>2</sub>Cl<sub>2</sub>/CS<sub>2</sub>, 297 K).**



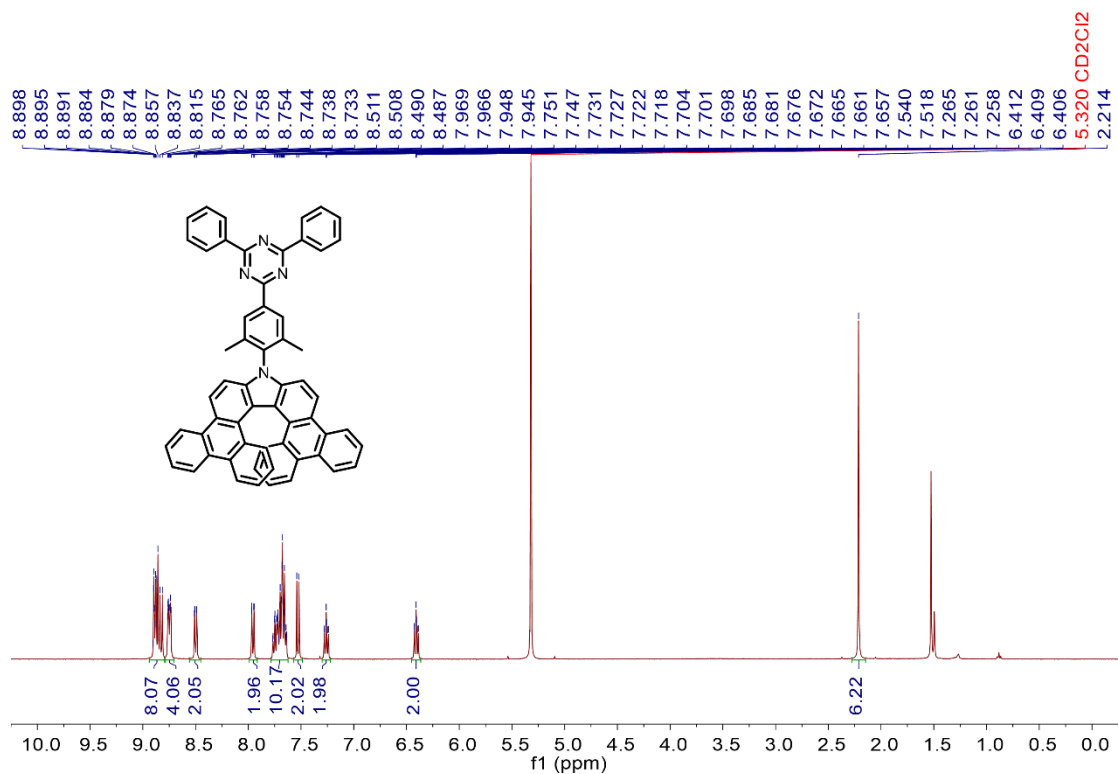


**Figure S15.** <sup>1</sup>H NMR spectrum of DMTrz-A7H (400 MHz, CD<sub>2</sub>Cl<sub>2</sub>, 297 K).

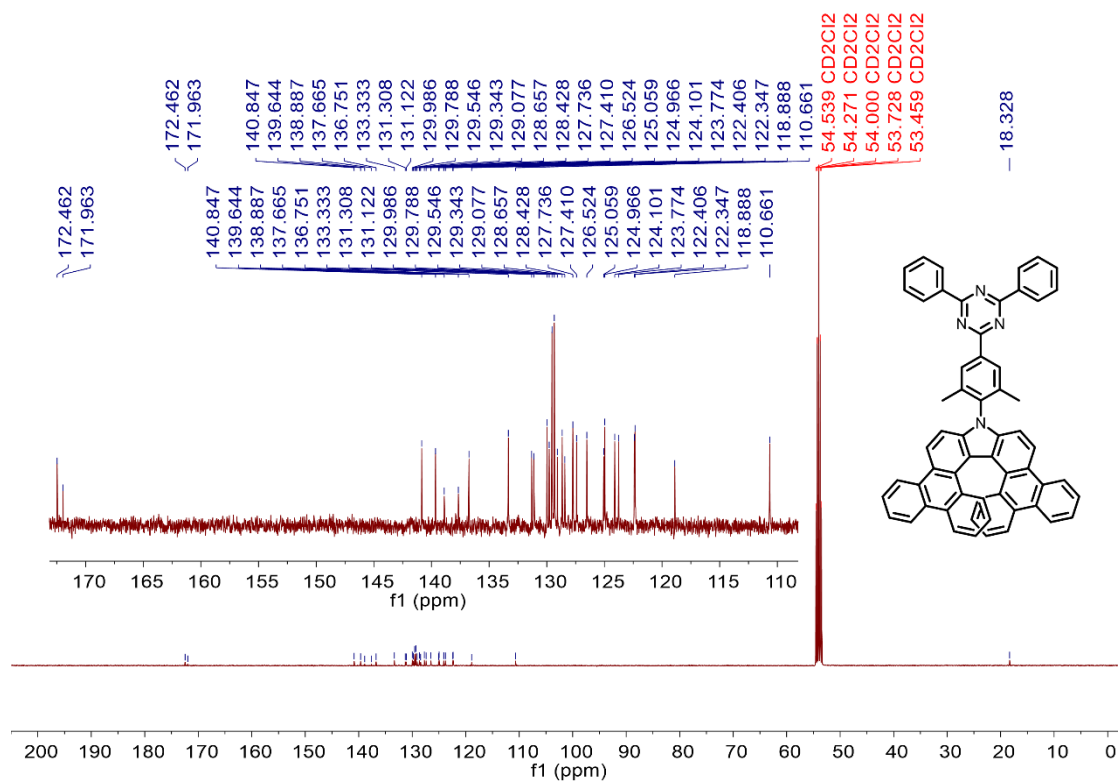


**Figure S16.** <sup>13</sup>C NMR spectrum of DMTrz-A7H (101 MHz, CD<sub>2</sub>Cl<sub>2</sub>, 297 K).

## 7. References

1. Maeda, C.; Nagahata, K.; Shirakawa, T.; Ema, T. *Angew. Chem. Int. Ed.* **2020**, *59*, 7813-7817.
2. Gaussian 09, Revision D.01, Frisch, M. J.; Trucks, G. W.; Schlegel, H. B.; Scuseria, G. E.; Robb, M. A.; Cheeseman, J. R.; Scalmani, G.; Barone, V.; Mennucci, B.; Petersson, G. A.; Nakatsuji, H.; Caricato, M.; Li, X.; Hratchian, H. P.; Izmaylov, A. F.; Bloino, J.; Zheng, G.; Sonnenberg, J. L.; Hada, M.; Ehara, M.; Toyota, K.; Fukuda, R.; Hasegawa, J.; Ishida, M.; Nakajima, T.; Honda, Y.; Kitao, O.; Nakai, H.; Vreven, T.; Montgomery, Jr., J. A.; Peralta, J. E.; Ogliaro, F.; Bearpark, M.; Heyd, J. J.; Brothers, E.; Kudin, K. N.; Staroverov, V. N.; Kobayashi, R.; Normand, J.; Raghavachari, K.; Rendell, A.; Burant, J. C.; Iyengar, S. S.; Tomasi, J.; Cossi, M.; Rega, N.; Millam, N. J.; Klene, M.; Knox, J. E.; Cross, J. B.; Bakken, V.; Adamo, C.; Jaramillo, J.; Gomperts, R.; Stratmann, R. E.; Yazyev, O.; Austin, A. J.; Cammi, R.; Pomelli, C.; Ochterski, J. W.; Martin, R. L.; Morokuma, K.; Zakrzewski, V. G.; Voth, G. A.; Salvador, P.; Dannenberg, J. J.; Dapprich, S.; Daniels, A. D.; Farkas, Ö.; Foresman, J. B.; Ortiz, J. V.; Cioslowski, J.; Fox, D. J. Gaussian Inc., Wallingford CT, 2013.
3. Lu, T.; Chen, F. *J. Comput. Chem.* **2012**, *33*, 580-592.
4. Humphrey, W.; Dalke, A.; Schulten, K. *J. Molec. Graphics* **1996**, *14*, 33-38.
5. Duan, C.; Zhang, J.; Xiang, J.; Yang, X.; Gao, X. *Angew. Chem. Int. Ed.* **2022**, *61*, e202201494
6. Ravat, P. *Chem. Eur. J.* **2021**, *27*, 3957-3967.